Electrochemical Evidences for Promoted Interfacial Reactions: The Role of Fe(II) Adsorbed onto γ-Al_2O_3 and TiO_2 in Reductive Transformation of 2-Nitrophenol

FANG-BAI LI,*,† LIANG TAO,†,‡,⊥ CHUN-HUA FENG,§ XIANG-ZHONG LI,∥ AND KE-WEN SUN†,‡,⊥

Guangdong Key Laboratory of Agricultural Environment Pollution Integrated Control, Guangdong Institute of Eco-Environmental and Soil Sciences, Guangzhou 510650, PR China, Guangzhou Institute of Geochemistry, Chinese Academy of Sciences, Guangzhou 510640, PR China, School of Chemistry and Chemical Engineering, South China University of Technology, Guangzhou 510640, PR China, Department of Civil and Structural Engineering, The Hong Kong Polytechnic University, Hong Kong, China, and Graduate University of Chinese Academy of Sciences, Beijing 100039, PR China

Received November 25, 2008. Revised manuscript received March 03, 2009. Accepted March 14, 2009.

This study was aimed at elucidating the role of adsorbed Fe(II) on minerals in the reductive transformation of 2-nitrophenol (2-NP) by using electrochemical methods. The studies of Fe(II) adsorption and 2-NP reduction kinetics showed that the identity of minerals such as γ-Al_2O_3 and TiO_2 and the solution pH were crucial factors to determine the Fe(II) adsorption behavior and to influence the rate constant (k) of 2-NP reduction. Furthermore, two electrochemical methods, cyclic voltammetry (CV) and electrochemical impedance spectrometry (EIS), were applied to characterize the Fe(II) reactivity with both the mineral-coated and mineral-free electrodes. The electrochemical evidence confirmed that the peak oxidation potential (E_P) of complex Fe(II) can be significantly affected by the solution pH; the enhanced reductive transformation of 2-NP can be related to the reduced E_P of surface-complex Fe(II) and the reduced charge transfer resistance (R_{CT}) of the Fe(III)/Fe(II) couple. All these relationships were studied quantitatively. At pH 6.7, the measured E_P and R_{CT} decreased in the order TiO_2/GC < γ-Al_2O_3/GC < GC (E_P, 0.140 < 0.190 < 0.242 V; R_{CT}, 0.30 < 0.41 < 0.78 kΩ), while the 2-NP reduction on different minerals were in the order TiO_2 > γ-Al_2O_3 > nonmineral ($k \times 10^{-2}$, 7.91 > 0.64 > 0.077 min^{-1}).

Introduction

Ferrous iron [Fe(II)] adsorption onto mineral surfaces is an important environmental process because the surface-complex Fe(II) enables a facile reductive transformation of organic/inorganic pollutants in contaminated soils (*1*−*6*). Studies on the interaction between Fe(II) and mineral surfaces have attracted increasing attention to understand the contribution of surface species to the enhanced reactivity (*1, 7*−*15*). A general consensus is that the mineral surface provides hydroxyl groups to stabilize Fe(II), leading to the formation of surface-complex Fe(II) species such as ≡$SOFe^+$ and ≡$SOFeOH^0$ with lower redox potential compared to aqueous Fe(II) species. The negative shift of the redox potential proved to be indicative of the enhancement of Fe(II) reactivity (*16, 17*). However, despite the above well-recognized conclusion, there is a lack of experimental evidence regarding the magnitude of redox potential response to the variation in the identity of surface-complex Fe(II) species and the quantitative measurements of the Fe(II)-to-Fe(III) electron transfer rate. In order to investigate these insights, this study attempted to establish an electrochemical system to characterize the redox behavior and the electron transfer process of the adsorbed Fe(II) in the interfacial phase. Cyclic voltammetry (CV) and electrochemical impedance spectrometry (EIS), which are powerful tools (*18*−*20*) in electrochemistry, were exploited to study the electron transfer on a solid electrode.

To compare the electrochemical behaviors of different reactive Fe(II) surface complexes, γ-Al_2O_3 and TiO_2 as important classes of Fe-free soil minerals (*21*−*23*) were selected to allow the adsorption of Fe(II) over a wide range of pH. Some iron minerals in soil such as goethite and hematite were excluded from this study because Fe(II) cannot only be adsorbed onto but also react with the underlying Fe(III) oxides (*24*). This might add complexity to the media and make it difficult to study the role of adsorbed Fe(II) in pollutant reduction. By use of the diffuse double layer model (DDL) (*25*), the dominant surface species (*16, 17*) on each individual mineral and its concentration were predicted. Meanwhile, the mineral-modified glass carbon (GC) electrodes were prepared to investigate the electrochemical response of the Fe(II) surface species. 2-Nitrophenol (2-NP) was employed as a model pollutant to investigate its reductive transformation by the surface-complex Fe(II) under various experimental conditions.

This study has been focused on the establishment of relationships among the amounts of the adsorbed Fe(II) surface species, the kinetics of 2-NP transformation, and the electrochemical behavior of the Fe(II) surface complexes on the γ-Al_2O_3 and TiO_2 minerals. For comparison, kinetic and electrochemical studies with the aqueous Fe(II) species were also investigated.

Experimental Section

Chemicals. The model pollutant 2-NP, with a purity of >99.5%, was purchased from Acors. Detailed information on the other chemicals is presented in the Supporting Information.

Adsorption Study. Experiments on Fe(II) adsorption onto different minerals (γ-Al_2O_3 and TiO_2) were conducted in borosilicate glass serum bottles (effective volume = 20 mL) with aluminum crimps and Teflon-lined butyl rubber septa. Batch studies were conducted to access the influence of pH (from 4.0 to 8.0) on the extent of Fe(II) adsorption. To prevent any Fe(II) oxidation, all experiments were conducted inside an oxygen-free glovebox (model Bactron II, Anaerobic Chamber, 200 plate capacity) at 25 °C. The bottles containing 0.5 mM $FeSO_4$, 28 mM buffer, 200 mM NaCl, and 68.0 mg of mineral powders were then placed on a rotator at 200 rpm and 25 °C. Due to the high possibility of Fe(II) being oxidized

* Corresponding author phone: 86-20-87024721; fax: 86-20-87024123; e-mail: cefbli@soil.gd.cn.
† Guangdong Institute of Eco-Environmental and Soil Sciences.
‡ Chinese Academy of Sciences.
⊥ Graduate University of Chinese Academy of Sciences.
§ South China University of Technology.
∥ The Hong Kong Polytechnic University.

10.1021/es8033445 CCC: $40.75
Published on Web 04/16/2009

at circumneutral pH, the adsorption experiments at pH ≥6.5 were conducted with continuously bubbled nitrogen rather than on a rotator. The flow rate of nitrogen was 90 mL min^{-1}, which allows for the sufficient stirring of the suspension. After equilibrium, the final pH of each suspension was recorded before filtering (0.2 μm membrane filter). The acidified filtrate was then collected for the analysis of Fe(II) content.

Kinetics Study. The reduction of 2-NP was conducted under the conditions identical to adsorption experiments, except that 5.5 μM 2-NP was added to the reactor, and the kinetic measurements were conducted in a narrow pH range (from 5.5 to 7.0). The experimental setup is described in details in Scheme S1 of the Supporting Information.

Electrochemical Tests. Two mineral-modified glassy carbon (GC) electrodes were prepared using bare GC electrodes with a diameter of 3 mm, in which a GC electrode was first polished with emery paper followed by Al_2O_3 powders (particle sizes of 0.06 and 1 μm). Between the two polishing steps, the electrode was thoroughly rinsed with deionzed water. The polished electrode was successively cleaned with acetone and water in an ultrasonic bath for 10 min, respectively. Then the mineral slurry containing 5 mg of γ-Al_2O_3 or TiO_2 was prepared in a dilute Nafion solution (0.5 wt %, 250 μL) ultrasonically for 15 min. By using a microsyringe, aliquots (2 μL) of the above slurry was coated on the clean GC electrode and the electrode with the coating was dried in air for 30 min prior to use. The above two mineral-modified glassy carbon electrodes are named "γ-Al_2O_3/GC" and "TiO_2/GC", respectively, while a bare glassy carbon electrode is named "GC".

Electrochemical measurements were carried out in a standard three-electrode cell, consisting of a working electrode (γ-Al_2O_3/GC, TiO_2/GC, or GC), a counter electrode (platimum spiral), and a saturated calomel electrode (SCE) as the reference electrode [+0.24 V versus standard hydrogen electrode (SHE) at 25 °C]. If not mentioned otherwise, all the reported voltages were referred to SHE. Cyclic voltammgrams were recorded with an Autolab potentiostat (PGSTAT 30, Eco Chemie, The Netherlands) at a scan rate of 50 mV s^{-1}. The electrochemical cell was filled with a solution containing 3.0 mM $FeSO_4$ and 0.20 M NaCl buffered with 28 mM MES (2-morpholin-4-ylethanesulfonic acid, hydrate) or MOPS (3-*N*-morpholinopropansulfonic acid), and the solution pH was adjusted by adding diluted HCl or NaOH solution. High purity nitrogen gas was bubbled through the above electrolyte to remove dissolved oxygen. CV tests were performed under nitrogen atmosphere at 25 °C. EIS measurements were performed under the same conditions using an Autolab instrument. An ac voltage at 10 mV amplitude in the frequency range from 0.01 to 100 kHz under open circuit potential was applied in all measurements. The charge transfer resistance was predicted by modeling of the impedance curves with a simple Randles circuit (*18*).

Surface Complexation Modeling. MINEQL+ (Environmental Research Software) (*16, 17*) was used to calculate the equilibrium Fe(II) species in γ-Al_2O_3 and TiO_2 suspensions. The thermodynamic data required for the calculation are presented in Table S1 of the Supporting Information.

Analyses. The concentration of 2-NP was determined by high-performance liquid chromatography (HPLC). Fe(II) concentration was determined by the 1,10-phenanthroline method at 510 nm using a UV−visible spectrophotometer. All the detailed procedures are described in the Supporting Information.

Results and Discussion

Fe(II) Adsorption Behaviors Indicated by Surface-Complexation Modeling. The adsorption behaviors of Fe(II) onto minerals (γ-Al_2O_3 and TiO_2) are comparatively shown in parts A and B of Figure 1, respectively. It should be noted that Fe(II) adsorption onto two minerals exhibited similar pH-dependent patterns in which stronger Fe(II) adsorption occurred at higher pH values. However, the percentage of Fe(II) adsorption as a function of pH was heavily dependent upon the identity of minerals. For instance, the percentage of Fe(II) remaining in the TiO_2 suspension was markedly less than that in the γ-Al_2O_3 suspension over a pH range from 4.0 to 8.0, demonstrating that TiO_2 had the larger capacity for Fe(II) adsorption as compared to γ-Al_2O_3.

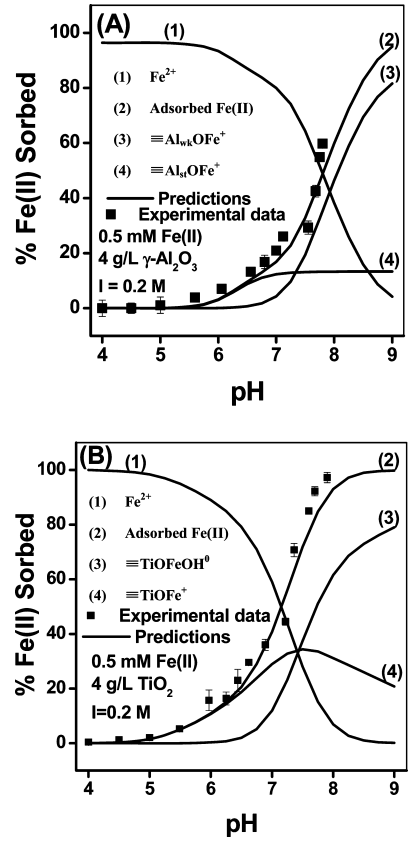

FIGURE 1. Fractional adsorption of Fe(II) onto γ-Al_2O_3 (A) and TiO_2 (B) as a function of pH by using stability constants provided in Table S1 of the Supporting Information. Adsorption conditions: 0.5 mM $FeSO_4$, 4.0 g L^{-1} mineral, pH 4−8, 0.2 M NaCl, and 25 °C.

A further analysis of the existing forms of adsorbed Fe(II) as well as their concentrations was performed using the diffuse double layer (DDL) surface complexation model (*25*). To ensure the model results can be consistent with the experimental adsorption data, both the single-site model (considering formation of $\equiv SOFe^{+}$ and $\equiv SOFeOH^{0}$ complexes at weak-binding sites) and the two-site model (considering formation of $\equiv SOFe^{+}$ complexes at both weak-binding and strong-binding sites) have been employed. In good agreement with the pioneering work done by Strathmann's group (*16, 17*), it was found that the single-site model was more suitable to quantify the concentrations of each Fe(II) surface species onto TiO_2, whereas the two-site model was more suitable for the γ-Al_2O_3 case. The distribution of individual surface-complex Fe(II) species as a function of pH in γ-Al_2O_3 and TiO_2 suspensions is included in Figure 1A,B. The calculation indicated that the Fe(II) adsorbed onto TiO_2 should be predominated by $\equiv TiOFe^{+}$ complex at pH <7.0 and the amount of $\equiv TiOFeOH^{0}$ complex should be gradually increased at pH >7.0, while the dominant Fe(II) species adsorbed onto γ-Al_2O_3 at pH <7.0 should be $\equiv Al_{st}OFe^{+}$ ($\equiv AlOFe^{+}$ at strong-binding sites), and a further increase of pH should increase both fractions of $\equiv Al_{st}OFe^{+}$ and $\equiv$Al-

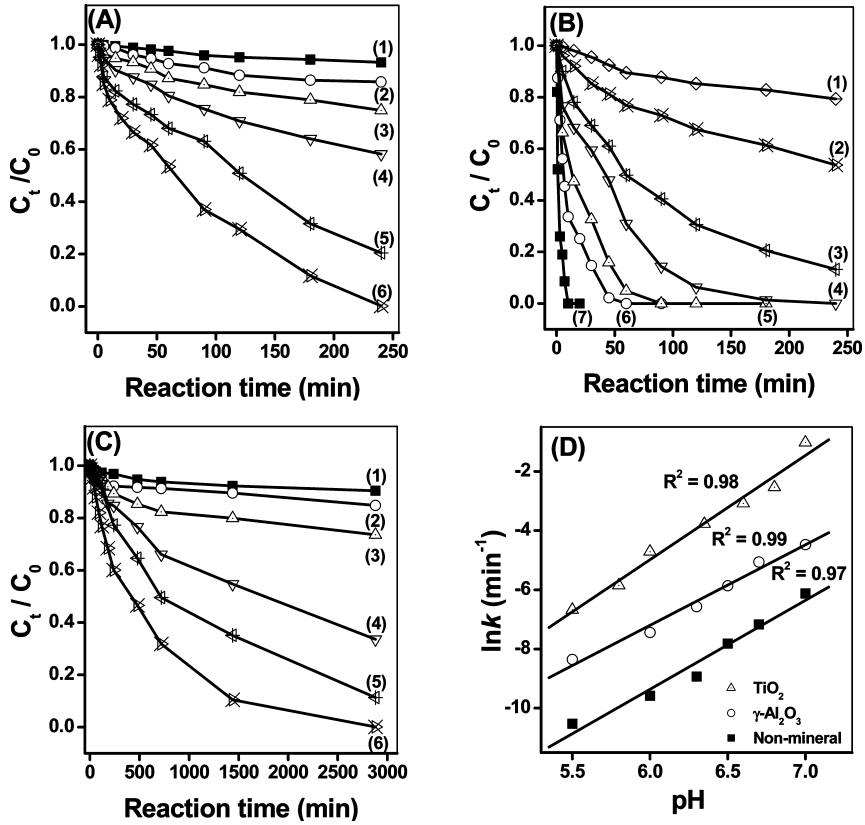

FIGURE 2. Effects of pH on the reductive transformation of 2-NP in γ-Al_2O_3 (A) and TiO_2 (B) suspensions and nonmineral solution (C). Plotting of ln *k* (the pseudo-first-order rate constant of 2-NP transformation) against pH (D). Reaction conditions: 0.5 mM $FeSO_4$, 5.5 μM 2-NP, 4.0 g L^{-1} mineral, pH = 5.5−7.0, 0.2 M NaCl, and T = 25 °C. Solution pH in γ-Al_2O_3 (A) suspension and nonmineral solution (C) was varied: (1) pH 5.5 (MES), (2) pH 6.0 (MES), (3) pH 6.3 (MES), (4) pH 6.5 (MES), (5) pH 6.7 (MOPS), and (6) pH 7.0 (MOPS). Solution pH in TiO_2 (B) was varied: (1) pH 5.5 (MES), (2) pH 5.8 (MES), (3) pH 6.0 (MES), (4) pH 6.4 (MES), (5) pH 6.6 (MOPS), (6) pH 6.8 (MOPS), and (7) pH 7.0 (MOPS).

TABLE 1. Relationships among the Concentrations of the Predicted Active Fe(II) Surface Species, the Kinetics of 2-NP Transformation, and the Electrochemical Parameters[a]

mineral surface	TiO_2	γ-Al_2O_3	nonmineral
active surface-complex Fe(II) species and its concentration (μM) [b]	$\equiv TiOFe^+$, 111.2	$\equiv Al_{st}OFe^+$, 56.0	–
peak oxidation potential (E_P /V) [c]	0.140	0.190	0.242
Fe(II)-to-Fe(III) electron transfer resistance (R_{CT}/kΩ) [d]	0.30	0.41	0.78
rate constant of 2-NP reduction ($k \times 10^{-2}$/min^{-1}) [e]	7.91	0.64	0.077

[a] The pH was controlled at 6.7 in 0.2 M NaCl and 28 mM MOPS solution. [b] Data from Figure 1. [c] Data from Figure 3. [d] Data from Figure 4. [e] Data from Figure 2.

$_{wk}OFe^+$ ($\equiv AlOFe^+$ at weak-binding sites). At pH >7.0, the extent of the $\equiv Al_{st}OFe^+$ should approach a stable value and the amount of $\equiv Al_{wk}OFe^+$ should exceed that of $\equiv Al_{st}OFe^+$. The predicted dominant Fe(II) surface complexes at pH 6.7 ($\equiv Al_{st}OFe^+$ and $\equiv TiOFe^+$, corresponding to γ-Al_2O_3 and TiO_2 minerals, respectively) are listed in Table 1.

Reductive Transformation of 2-NP by Adsorbed Fe(II). The kinetics of 2-NP reduction by adsorbed Fe(II) was evaluated by varying the experimental conditions. The adsorption of 2-NP onto different minerals under all the conditions was very low, as shown in Figure S1 of the Supporting Information; thus, the contribution of 2-NP adsorption to its reactivity could be neglected at the investigated pH values. On the other hand, the pH effect on Fe(II) reactivity is remarkable. As discussed above, pH played a tremendous role in affecting the adsorption of Fe(II) onto minerals (Figure 1). According to the literature (*4, 10, 12*), the amount of adsorbed Fe(II) on the mineral surface was indeed a crucial factor affecting the reduction rate of organic pollutants. The impact of pH on the reductive transformation of 2-NP was accordingly investigated in the γ-Al_2O_3 and TiO_2 suspensions with the same initial Fe(II) concentration but different pH. The results demonstrated the dependences of 2-NP degradation on the solution pH, as shown in Figure 2A,B. For kinetic comparison, a set of control tests was also conducted under the same experimental condition, but in aqueous solution without any minerals as a homogeneous reaction system, and the relevant results are comparatively illustrated in Figure 2C. Notably, the rates of 2-NP reduction by Fe(II) were significantly enhanced with an increase in pH in three cases. The kinetics of 2-NP reduction in both systems (heterogeneous and homogeneous) was found to follow the pseudo-first-order kinetic model under all experimental conditions (Supporting Information). The rate constant (k) values were then determined by fitting experimental data using the pseudo-first-order model. It is interesting to note that the k values increase exponentially with pH in all cases, as indicated by the three straight lines shown in Figure 2D.

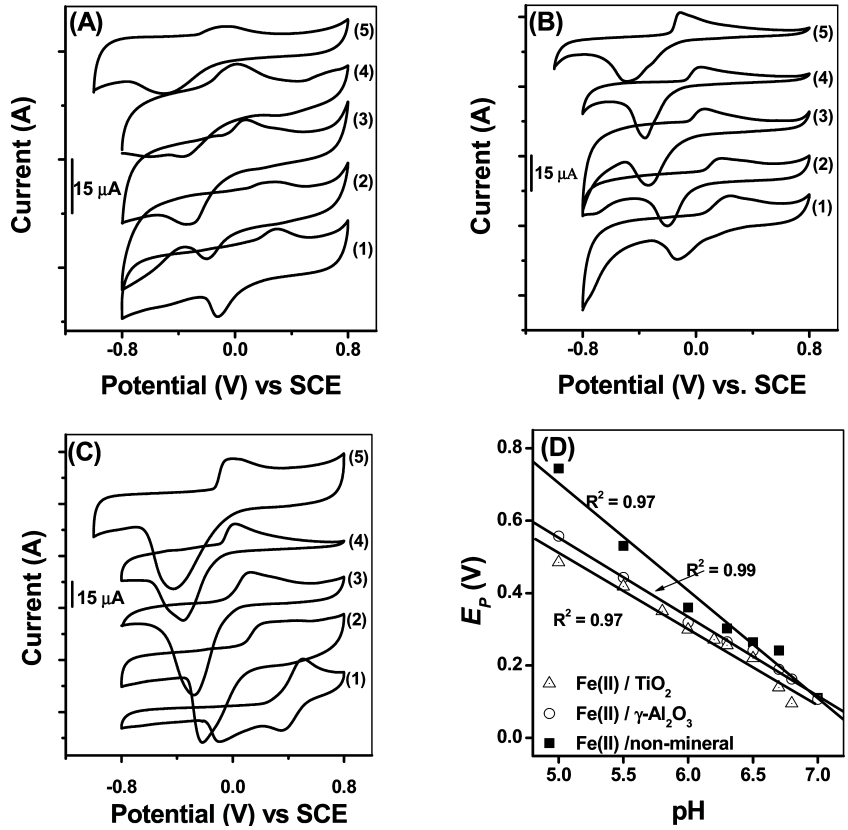

FIGURE 3. Cyclic voltammograms of adsorbed Fe(II) species on the γ-Al_2O_3/GC electrode (A), TiO_2/GC electrode (B), and GC electrode(C). The dependence of E_P (peak oxidation potential) on pH value (D) in γ-Al_2O_3 and TiO_2 suspensions and nonmineral solution, respectively. Electrochemical measurements were conducted in the cell (25 mL) containing 3.0 mM $FeSO_4$, 0.2 M NaCl solution, and 28 mM buffer at 25 °C. The mineral loading was estimated to be 2×10^{-3} g L^{-1}. Solution pH was varied: (1) pH 5.0, (2) pH 5.5, (3) pH 6.0, (4) pH 6.5, and (5) pH 6.7. The scan rate was 50 mV s^{-1}.

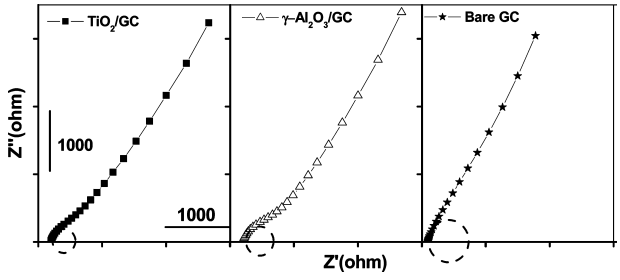

FIGURE 4. Impedance diagrams (Nyquist representation) measured at open circuit voltage for mineral-modified glassy carbon (GC) electrodes in the presence of 3.0 mM $FeSO_4$, 0.2 M NaCl, and 28 mM MOPS, at pH 6.7 and 25 °C.

By comparison, it was found that the addition of minerals could greatly facilitate the 2-NP reduction and the reduction rate was strongly dependent on the identity of minerals (Figure S2 of the Supporting Information). Figure 2D shows that the resultant k values of 2-NP reduction at the fixed pH in the presence/absence of minerals can be ranked from low to high as nonmineral < γ-Al_2O_3 < TiO_2, while the k values of 2-NP reduction on TiO_2 surface were found to be slightly more sensitive to the pH change than the other two cases. A further comparison of k normalized to the amount of adsorbed Fe(II) was performed for TiO_2 and γ-Al_2O_3. Results (Figure S3 of the Supporting Information) indicated that Fe(II) adsorbed onto TiO_2 may be more reactive than Fe(II) adsorbed onto γ-Al_2O_3 for the reductive transformation of 2-NP.

Electrochemical Behaviors of Adsorbed Fe(II) on the Mineral-Modified Electrodes. Given the homemade mineral-modified electrodes including γ-Al_2O_3/GC and TiO_2/GC, electrochemical characterizations (e.g., CV and EIS) were performed to evaluate the Fe(II)-to-Fe(III) electron transfer behaviors of adsorbed Fe(II). In particular, voltammograms obtained for the adsorbed Fe(II) on the modified GC electrodes provide direct evidence of the change of redox potentials. Parts A, B, and C of Figure 3 illustrate the pH effect on the redox behavior of the surface-complex Fe(II) and aqueous Fe(II) species on γ-Al_2O_3, TiO_2, and nonmineral, respectively. Clearly, all the voltammograms exhibited a pair of peaks: an anodic oxidation peak for Fe(II) at potentials ranging from −0.1 to 0.6 V (versus SCE) and a cathodic reduction peak for Fe(III) at potentials ranging from −0.6 to −0.1 V (versus SCE). Consistent with the theoretical results (*16*), both peaks shift toward more negative direction with the increase of pH. For instance, when pH was modulated from 5.5 to 6.7, the peak oxidation potential (denoted as E_P) of Fe(II) adsorbed onto γ-Al_2O_3 significantly decreased from 0.317 to −0.051 V (versus SCE). The linear E_P reduction against pH was found in three sets of reactions on the γ-Al_2O_3/GC, TiO_2/GC, and GC electrodes. In the meantime, it can be seen that at any fixed pH, E_P values of γ-Al_2O_3/GC and TiO_2/GC electrodes were significantly lower than that of GC electrode due to the Fe(II) adsorption onto these minerals. For instance, the measured E_P for TiO_2, γ-Al_2O_3, and nonmineral at pH 6.7 was 0.140, 0.190, and 0.242 V (versus SHE), respectively (Figure 3D and Table 1). Furthermore, it can be seen that the E_P value of GC electrode decreased faster than the others, while pH was increased. These results indicate that decrease of redox potential due to the Fe(II) adsorption onto the minerals is more significant in the low pH range rather than in the high pH range.

In order to better understand the mechanism of the promoted interfacial reactions by the surface-complex Fe(II)

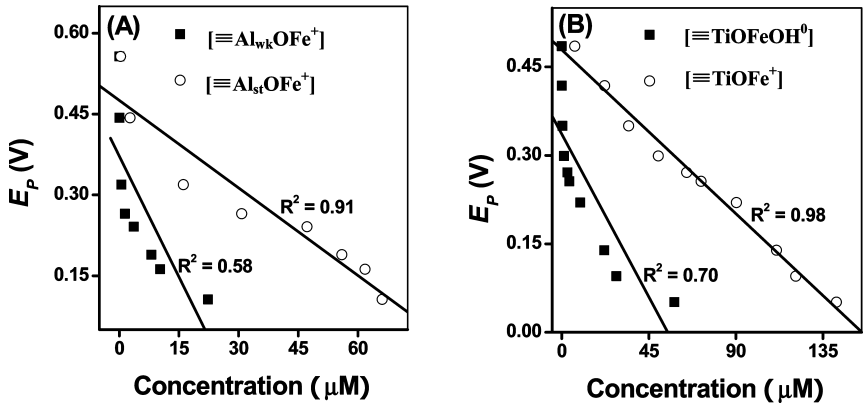

FIGURE 5. Correlation scatter plots for the dependence of E_P versus different surface-complex Fe(II) species in γ-Al_2O_3 (A) and TiO_2 (B) suspensions, respectively.

species, an attempt was made to examine the kinetic parameter of electrons transferring from Fe(II) to Fe(III). The electrochemical impedance method, a useful tool to study the interfacial property of modified electrodes, was then used to characterize the electron-transfer rate (*18*−*20*). More information on this technique is included in the Supporting Information. In consideration of different surface-complex Fe(II) available on different minerals, it would be meaningful if the different impedance signals can be detected. Figure 4 shows the Nyquist plots of bare GC electrode, γ-Al_2O_3/GC, and TiO_2/GC electrodes in the Fe(II)-containing solution. All the Nyquist curves exhibited similar impedance behaviors. A curved portion observed in the high-frequency region should be associated with the redox process of Fe(III)/Fe(II) couple involved on each electrode; a straight line observed in the low-frequency region should be attributed to the mass transport of redox species. However, the length of the curved region, by fitting with a circle, was clearly different among all the electrodes. The electron transfer resistance of the Fe(III)/Fe(II) couple can be estimated by the amplitude of the semicircle in the high-frequency region (*18*−*20*). Obviously, it can be seen that all the modified electrodes showed smaller circles in comparison with the bare GC electrode, indicating the higher electron transfer rates on the modified electrodes. In addition, the TiO_2/GC electrode gave rise to the smallest semicircle, indicating that Fe(II) adsorbed onto TiO_2 surfaces can be transferred to Fe(III) at the fastest rate.

Relationship between the Distribution of Surface-Complex Fe(II) and Electrochemically Obtained E_P. The apparent E_P values were obtained from the electrochemical cell that contained much lower mineral loading compared to that used in the adsorption experiments. Figure S5 of the Supporting Information revealed that the predicted distribution of surface-complex Fe(II) was linearly dependent on mineral loading. This suggests that it should be acceptable to correlate the electrochemically obtained parameters with the data collected from the adsorption and kinetic studies.

Adsorption studies revealed that modulating pH can significantly change the extent of Fe(II) adsorbed onto different minerals (Figure 1), as increasing pH facilitates surface deprotonation reactions and thus leads to the production of surface-complex Fe(II) (*16, 17*). Our electrochemical studies demonstrated that the measured E_P was also highly dependent on pH (Figure 3). Thus, the association between the apparent E_P and the concentration of surface-complex Fe(II) on each mineral can be established (Figure 5). A good linear relationship of E_P with the concentration of $\equiv Al_{st}OFe^+$ (R^2 = 0.91) or $\equiv TiOFe^+$ (R^2 = 0.98) was accordingly obtained. In contrast, poor linear dependence of E_P on $\equiv Al_{wk}OFe^+$ ($R^2 = 0.58$) or $\equiv TiOFeOH^0$ ($R^2 = 0.70$) was revealed. These observations could be understood on the basis of the fact that the dominant surface species on γ-Al_2O_3 and TiO_2 in the investigated pH range (from 5.5 to 7.0) was $\equiv Al_{st}OFe^+$ and $\equiv TiOFe^+$, respectively (Figure 1). Taking into account the close relationship between E_P and the reaction kinetics, it is likely that $\equiv Al_{st}OFe^+$ and $\equiv TiOFe^+$ should be the active surface complexes Fe(II) with respect to γ-Al_2O_3 and TiO_2 surfaces. These active species might predominantly influence the E_P values, which further correspond to different reaction rates.

Relationships between the Reactivity of Fe(II) Species and Electrochemical Parameters (E_P and R_{CT}). Previous studies have reported that the enhanced reactivity of Fe(II) species associated with solid phases was attributed to the negative shift of redox potential of the Fe(III)/Fe(II) couple, but most of the interpretation only relied on theoretical calculations (*9, 11*). It is the first time that this study provides the direct electrochemical evidence to confirm the previous understanding of interfacial reactions involving adsorbed Fe(II). Both E_P (peak oxidation potential resulted from CV characterization) and R_{CT} (electron transfer resistance resulted from EIS characterizations) can be regarded as important indicators with regard to the reactivity of Fe(II) species on minerals.

According to the linear free-energy relationship (LFER) (*16, 17, 25*), which correlates the thermodynamic change of Gibbs free energy (ΔG) of Fe(III)/Fe(II) couple to the kinetic rate constant, the low E_P value (corresponding to the low ΔG) is beneficial to enhance the reaction rate of pollutant transformation by Fe(II). This relationship can be experimentally demonstrated and is shown in Figure S6 of the Supporting Information. The pronounced effect of E_P on ln k is consistent for both the homogeneous and heterogeneous systems in that the negative shift of E_P resulted from elevated pH accounts for the enhanced rates of 2-NP reduction. In addition, at the fixed pH, the E_P values with respect to different systems were also different, resulting in different reaction rates. Table 1 lists the specific values of k and E_P obtained from two types of minerals as well as from homogeneous system at pH 6.7. Notably, the k value increases in the order nonmineral < γ-Al_2O_3 < TiO_2; on the other hand, the E_P value increases in the contrary order TiO_2 < γ-Al_2O_3 < nonmineral. Although a linear association between ln k and E_P was demonstrated for all cases, plotting of ln k versus E_P did not collapse onto a single line. This indicates that E_P, known as the thermodynamic characteristic of the Fe(III)/Fe(II) couple, is not the exclusive factor to determine the reaction kinetics. The Fe(II)-to-Fe(III) electron transfer kinetics instead is another important parameter that one needs to examine.

Modeling of impedance curves with the Randles equivalent circuit for different minerals allows the determination of R_{CT} with respect to Fe(II)-to-Fe(III) reactions (Figure S4 of the Supporting Information). As a typical example, the R_{CT} values were quantified at pH 6.7 for all types of minerals. As

presented in Table 1, the predicted R_{CT} for the Fe(II)-to-Fe(III) reaction on the TiO_2/GC electrode is 0.30 kΩ, which is 62% less than that on the mineral-free (GC) electrode and 27% less than that on the γ-Al_2O_3/GC electrode. The trend of the decline in R_{CT} is well-consistent with the order of the increase in k.

Environmental Implications. 2-NP reduction by Fe(II) mainly depends on three key issues: (1) the amount of Fe(II) (either adsorbed Fe(II) complex or dissolved Fe(II) ions as a reductant to react with 2-NP), (2) E_P (from a thermodynamic point of view, lower E_P can enhance the 2-NP reduction reaction, which is mainly affected by increasing pH and slightly affected due to the adsorption of Fe(II) on the mineral surface), and (3) transfer rate (R_{CT}) of Fe(III)/Fe(II) couple on the minerals, which depends on the characteristics of minerals. From this study, we can understand that the electrochemical approach could be used as a useful tool to quantitatively determine the above two key factors of E_P and R_{CT} under various reaction conditions and with different minerals. This method will contribute to the characterization of the Fe(II) complex (including surface complex and aqueous complex) involved reactions for the reductive transformation of contaminants in real subsurface environments.

Acknowledgments

The work was financially supported by the National Natural Science Foundation of PR China (No. 40771105 and 20577007). We are grateful to the anonymous reviewers for their constructive and helpful comments. We also thank Prof. T. Strathmann for his valuable comments on the discrepancy problem between the measured adsorbed Fe(II) concentrations and model results. Thanks also go to Dr. William D. Schecher, who updated us the new MINEQL program (version 4.62.1).

Supporting Information Available

Sections S1−S9, Table S1, Scheme S1, and Figures S1−S6 are included. This material is available free of charge via the Internet at http://pubs.acs.org.

Literature Cited

(1) Li, F. B.; Wang, X. G.; Li, Y. T.; Liu, C. S.; Zeng, F.; Zhang, L. J.; Hao, M. D.; Ruan, H. D. Enhancement of the reductive transformation of pentachlorophenol by polycarboxylic acids at the iron oxide−water interface. *J. Colloid Interface Sci.* **2008**, *321*, 332–341.

(2) Rügge, K.; Hofstetter, T. B.; Haderlein, S. B.; Bjerg, P. L.; Knudsen, S.; Zraunig, C.; Mosbæk, H.; Christensen, T. H. Characterization of predominant reductants in an anaerobic leachate-contaminated aquifer by nitroaromatic probe compounds. *Environ. Sci. Technol.* **1998**, *32*, 23–31.

(3) Yan, L. B.; Bailey, G. W. Sorption and abiotic redox transformation of nitrobenzene at the smectite−water interface. *J. Colloid Interface Sci.* **2001**, *241*, 142–153.

(4) Stumm, W.; Sulzberger, B. The cycling of iron in natural environments—Considerations based on laboratory studies of heterogeneous redox processes. *Geochim. Cosmochim. Acta* **1992**, *56*, 3233–3257.

(5) Klausen, J.; Trober, S. P.; Haderlein, S. B.; Schwarzenbach, R. P. Reduction of substituted nitrobenzenes by Fe(II) in aqueous mineral suspensions. *Environ. Sci. Technol.* **1995**, *29*, 2396–2404.

(6) Klupinski, T. P.; Chin, Y. P.; Traina, S. J. Abiotic degradation of pentachloronitrobenzene by Fe(II): Reactions on goethite and iron oxide nanoparticles. *Environ. Sci. Technol.* **2004**, *38*, 4353–4360.

(7) Rush, J. D.; Koppenol, W. H. The reaction between ferrous polyaminocarboxylate complexes and hydrogen peroxide: An investigation of the reaction intermediates by stopped flow spectrophotometry. *J. Inorg. Biochem.* **1987**, *29*, 199–215.

(8) Buerge, I. J.; Hug, S. J. Influence of organic ligands on chromium(VI) reduction by iron(II). *Environ. Sci. Technol.* **1998**, *32*, 2092–2099.

(9) Strathmann, T. J.; Stone, A. T. Reduction of oxamyl and related pesticides by Fe^{II}: Influence of organic ligands and natural organic matter. *Environ. Sci. Technol.* **2002**, *36*, 5172–5183.

(10) Hiemstra, T.; Riemsdijk, W. H. Adsorption and surface oxidation of Fe(II) on metal (hydr)oxides. *Geochim. Cosmochim. Acta* **2007**, *71*, 5913–5933.

(11) Strathmann, T. J.; Stone, A. T. Reduction of the pesticides oxamyl and methomyl by Fe^{II}: Effect of pH and inorganic ligands. *Environ. Sci. Technol.* **2002**, *36*, 653–661.

(12) Strathmann, T. J.; Stone, A. T. Mineral surface catalysis of reactions between Fe^{II} and oxime carbamate pesticides. *Geochim. Cosmochim. Acta* **2003**, *67*, 2775–2791.

(13) Pecher, K.; Haderlein, S. B.; Schwarzenbach, R. P. Reduction of polyhalogenated methanes by surface-bound Fe(II) in aqueous suspensions of iron oxides. *Environ. Sci. Technol.* **2002**, *36*, 1734–1741.

(14) Hofstetter, T. B.; Heijman, C, G.; Haderlein, S. B.; Holliger, C.; Schwarzenbach, R. P. Complete reduction of TNT and other (poly)nitroaromatic compounds under iron-reducing subsurface conditions. *Environ. Sci. Technol.* **1999**, *33*, 1479–1487.

(15) Colon, D.; Weber, E. J.; Anderson, J. L.; Winget, P.; Suarez, L. A. Reduction of nitrosobenzenes and *N*-hydroxylanilines by Fe(II) species: Elucidation of the reaction mechanism. *Environ. Sci. Technol.* **2006**, *40*, 4449–4454.

(16) Nano, G. V.; Strathmann, T. J. Ferrous iron sorption by hydrous metal oxides. *J. Colloid Interface Sci.* **2006**, *297*, 443–454.

(17) Nano, G. V.; Strathmann, T. J. Application of surface complexation modeling to the reactivity of iron(II) with nitroaromatic and oxime carbamate contaminants in aqueous TiO_2 suspensions. *J. Colloid Interface Sci.* **2008**, *321*, 350–359.

(18) Bard, A. J.; Faulkner, L. R. *Electrochemical Methods*; John Wiley & Sons Inc.: New York,1980.

(19) Liu, H.; Cheng, S. A.; Wu, M.; Wu, H. J.; Zhang, J. Q.; Li, W. Z.; Cao, C. N. Photoelectrocatalytic degradation of sulfosalicylic acid and its electrochemical impedance spectroscopy investigation. *J. Phys. Chem. A.* **2000**, *104*, 7016–7020.

(20) Li, H.; Li, X. Z.; Leng, Y. J.; Li, W. Z. An alternative approach to ascertain the rate-determining steps of TiO_2 photoelectrocatalytic reaction by electrochemical impedance spectroscopy. *J. Phys. Chem. B.* **2003**, *107*, 8988–8996.

(21) Schoonen, M. A. A.; Xu, Y.; Strongin, D. R. An introduction to geocatalysis. *Geochem. Explor.* **1998**, *62*, 201–215.

(22) Rhoton, F. E.; Bigham, J. M.; Lindbo, D. L. Properties of iron oxides in streams draining the loess uplands of Mississippi. *Appl. Geochem.* **2002**, *17*, 409–419.

(23) Swearingen, C.; Macha, S.; Fitch, A. Leashed ferrocenes at clay surfaces: Potential applications for environmental catalysis. *J. Mol. Catal. A* **2003**, *199*, 149–160.

(24) Williams, A. G. B.; Scherer, M. M. Spectroscopic evidence for Fe(II)−Fe(III) electron transfer at the iron oxide−water interface. *Environ. Sci. Technol.* **2004**, *38*, 4782–4790.

(25) Dzombak, D. A.; Morel, F. M. M. *Surface Complexation Modeling: Hydrous Ferric Oxide*; Wiley-Interscience: New York, 1990.

ES8033445